207

Boundary layer growth on two circular cylinders

P.G. KALITZOVA-KURTEVA and Z.D. ZAPRYANOV*
*Department of Fluid Mechanics, Institute of Mechanics and Biomechanics, BAS, 1113 Sofia, Bulgaria (*author for correspondence)*

Abstract. This paper deals with the problem of boundary layer growth on two circular cylinders in a flow with large Reynolds and Strouhal numbers. Analytic solutions for the stream function of the inner and outer flow field are obtained to the second order by using the method of matched asymptotic expansions. The dependence of the movement of the detachment points and the drag coefficients of the two cylinders on (i) the distance between them, (ii) the ratio of their radii, (iii) the Reynolds number and (iv) the acceleration parameter of the flow is investigated. The results obtained indicate that the mutual hydrodynamic interaction between two cylinders leads to some new relations and findings.

1. Introduction

This paper is an investigation having the overall objective of obtaining an approximate solution for the problem of unsteady motion of two bodies in a viscous fluid. An important class of such fluid flows is that in which the bodies start to move from rest either impulsively or with acceleration.

Rayleigh [1] solved the problem when an infinite plate is moved impulsively in its own plane at a speed U_0 in a viscous fluid. In 1950, Howart [2] discussed another problem of the Rayleigh type—a semi-infinite flat plate is moved impulsively parallel to its edge in a viscous fluid. The motion of a wedge in a viscous fluid has been studied by Hasimoto [3] and Sowerby and Cooke [4]. An exact solution for the problem of an impulsive motion of a circular cylinder parallel to its generators is due to Carslaw and Jaeger [5]. Generalizing their solution, Batchelor [6] considered the impulsive motion of a cylinder of arbitrary cross-section parallel to its generators.

The problem of the growth of the boundary layer on a body which is started from rest in an infinite incompressible viscous fluid has been investigated by many authors. The first step was made by Blasius [7] who considered the case of an impulsively started circular cylinder as well as the case of a uniformly accelerated one. Goldstein and Rosenhead [8] extended his solution to the next approximation. Görtler [9] and Watson [10] generalized that problem by assuming that the velocity of the cylinder varies as some power of time. All the above investigations were based on Prandtl's equations.

It is well known that Prandtl's boundary layer theory, which is the foundation for development of the general viscous flow theory, gives us the first-order approximation to the solution of the Navier–Stokes equations for the limit of large Reynolds numbers. However, many flows that occur in modern technology possess properties that cannot be treated within the framework of Prandtl's approximation because it neglects the surface curvature and the displacement of the external flow by the boundary layer thickness.

On the basis of high-order boundary layer theory short-time solutions for flows past a

cylinder which starts from rest with several different prescribed motions have been presented by Wang [11, 12], Zapryanov [13], Slavchev [14], Z. Zapryanov and P. Kalitzova-Kurteva [15], Simeonov [16].

For a long time, the flows in many engineering applications were assumed to be steady. Unsteady phenomena are worth studying only if they depart substantially from the quasi-steady state. An important class of such problems involves devices as the helicopter rotor, cascades of blades of turbomachinery and the ship propeller. Such devices operate in an unsteady environment and cannot be treated as quasi-steady. The lifting characteristics of an airfoil or drag characteristics of a blunt body encounter smooth or sudden changes in their environment and can not be considered as quasi-steady as well.

Another class of important unsteady engineering problems involves the study of the flow through heat exchangers in reactors. The most important elements of heat exchangers are circular tubes (cylinders) [17]. In some cases the situation is such that the cross viscous flow past two cylinders has to be used [18]. It is of particular interest to investigate the formation and the initial stage of development of unsteady boundary layers around two circular cylinders which initiate translational motion from rest with a velocity varying as some power of time. The case of impulsively started profiles can be obtained as a special case. In order to investigate the mutual interactions between the boundary layers on the cylinders and the inviscid outer flow we have solved approximately (as in [19, 20]) the full Navier–Stokes equations by using the method of matched asymptotic expansions.

The early stages of viscous flows that start to move from rest either impulsively or with acceleration around two bodies contain valuable information of the flow properties. The character of the solution and its behaviour for small times is necessary input for the numerical calculations. That is why this kind of solution is essential in the study of unsteady flows and the thorough understanding of their properties [21].

2. Statement of the problem

Let us consider two parallel circular cylinders of radii a and b immersed in a viscous, incompressible fluid with kinematic viscosity ν and density ρ (see Fig. 1). It is assumed that the flow starts to move with linear velocity

$$V'(t) = U_0(t'/T_0)^\alpha , \qquad V(t) = V'(t)/U_0 = t^\alpha$$

in a direction parallel to the plane containing the axes of the cylinders and perpendicular to these axes. Here $\alpha \geq 0$ is a constant, t' denotes the dimensional time, T_0 and U_0 are the characteristic time and velocity respectively.

Due to the specific geometry of the two boundaries it is convenient to use bipolar co-ordinates (ξ, η), defined by the transformation

$$x' = c \sinh \eta /(\cosh \eta - \cos \xi) , \qquad y' = c \sin \xi /(\cosh \eta - \cos \xi) ,$$

where $0 \leq \xi < 2\pi$, $-\infty < \eta < \infty$ and $c > 0$ is the focal separation. Then the two cylinders external to each other can be defined by $\eta = \eta_1 < 0$ $(a = c|\text{cosech } \eta_1|)$ and $\eta = \eta_2 > 0$ $(b = c|\text{cosech } \eta_2|)$ [22]. The fluid region will be bounded by $\eta_1 < \eta < \eta_2$, $0 \leq \xi < 2\pi$ and at infinity $(\xi = 0, \eta = 0)$.

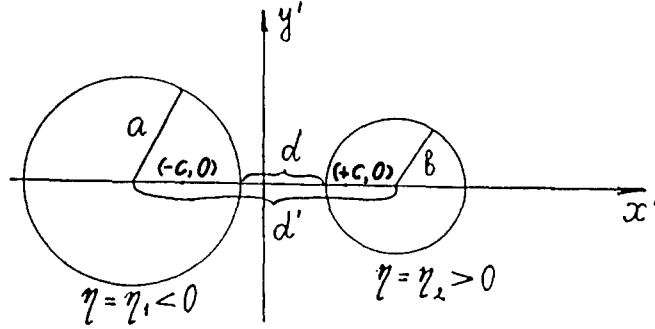*Fig. 1.* Schematic sketch of the problem.

Non-dimensional variables and parameters are introduced according to the scheme

$$x' = Lx , \qquad y' = Ly , \qquad t' = T_0 t , \qquad u' = U_0 u , \qquad v' = U_0 v ,$$

$$\psi' = U_0 L \psi , \qquad \mathrm{Re} = U_0 L / \nu , \qquad \mathrm{St} = L / U_0 T_0$$

where $L = a$ is a typical length.

We also assume [11, 12] large Reynolds and Strouhal numbers, so that

$$1/\mathrm{St} = 1/\nu' \, \mathrm{Re} = \varepsilon ,$$

where ε is a small parameter and ν' is a constant of order unity.

We concentrate our attention to small times, so we shall normalize t' by

$$T_0 = \varepsilon a / U_0 \quad \text{or} \quad t' = (\varepsilon a / U_0) t = (\varepsilon t) a / U_0 = T_1 a / U_0 ,$$

and therefore the dimensionless form of the equations of motion and continuity is

$$\frac{\partial u}{\partial t} + \varepsilon \left(\frac{u}{h} \frac{\partial u}{\partial \xi} + \frac{v}{h} \frac{\partial u}{\partial \eta} + \frac{uv}{h^2} \frac{\partial h}{\partial \eta} - \frac{v^2}{h^2} \frac{\partial h}{\partial \xi} \right)$$

$$= -\frac{1}{h} \frac{\partial p}{\partial \xi} - \frac{\varepsilon^2 \nu'}{h} \frac{\partial}{\partial \eta} \left\{ \frac{1}{h^2} \left[\frac{\partial}{\partial \xi} (hv) - \frac{\partial}{\partial \eta} (hu) \right] \right\} , \tag{1}$$

$$\frac{\partial v}{\partial t} + \varepsilon \left(\frac{u}{h} \frac{\partial v}{\partial \xi} + \frac{v}{h} \frac{\partial v}{\partial \eta} + \frac{uv}{h^2} \frac{\partial h}{\partial \xi} - \frac{u^2}{h^2} \frac{\partial h}{\partial \eta} \right)$$

$$= -\frac{1}{h} \frac{\partial p}{\partial \eta} - \frac{\varepsilon^2 \nu'}{h} \frac{\partial}{\partial \xi} \left\{ \frac{1}{h^2} \left[\frac{\partial}{\partial \eta} (hu) - \frac{\partial}{\partial \xi} (hv) \right] \right\} , \tag{2}$$

$$\frac{\partial}{\partial \xi} (hu) + \frac{\partial}{\partial \eta} (hv) = 0 , \tag{3}$$

where u, v are velocity components, $h = c/a(\cosh \eta - \cos \xi)$ and the pressure p' is normalized with respect to $\rho U_0^2 \, \mathrm{St}$.

If we introduce the Stokes stream function, such that

$$u = h^{-1} \, \partial \Psi / \partial \eta \,, \qquad v = -h^{-1} \, \partial \Psi / \partial \xi \,, \tag{4}$$

the equation of continuity will automatically be satisfied.

During the initial interval of time an inviscid potential flow prevails throughout the entire flow field, as it is shown in [11] for one cylinder. By the method of separation variables [23] the stream function for irrotational flow around two circular cylinders is found. So in terms of the stream function, the initial and boundary conditions for the problem considered are

$$\Psi = 0 \quad \text{for } t \leq 0 \,, \tag{5}$$

$$\Psi = t^{\alpha} \, \sinh|\eta_1| \Big\{ \sin \, \xi / (\cosh \eta - \cos \xi) + \sum_{k=1}^{\infty} \, [2 \exp(-k\eta_2) \sinh[k(\eta - \eta_1)]]$$

$$+ 2 \exp(k\eta_1) \sinh[k(\eta_2 - \eta)]] \sin k\xi / \sinh[k(\eta_1 - \eta_2)] \Big\} \quad \text{as } t \to 0^+ \,, \tag{6}$$

$$\Psi = 0 = \partial \Psi / \partial \eta \quad \text{at } \eta = \eta_1 \quad \text{and} \quad \eta = \eta_2 \,, \quad t > 0 \,, \tag{7}$$

$$\Psi \sim t^{\alpha} \, \sinh|\eta_1| \sin \, \xi / (\cosh \eta - \cos \xi) \quad \text{as } \xi^2 + \eta^2 \to 0 \,, \quad t > 0 \,. \tag{8}$$

3. Solution of the problem

In order to solve the problem (1)–(8) we have used the method of inner and outer expansions. In this method the region around the cylinders is divided into three separate but overlapping regions and an appropriate perturbation scheme relevant for each region is considered. Since the changes along the cylinders are much smaller than the changes normal to them, we magnify the normal co-ordinate η, as in the classical boundary layers,

$$\zeta = (\eta - \eta_1)/\varepsilon \,, \qquad \bar{\zeta} = (\eta_2 - \eta)/\varepsilon \,. \tag{9}$$

In the region of the boundary layer around the cylinder $\eta = \eta_1$ we assume the following asymptotic expansions:

$$u = u_1 + \varepsilon u_2 + \cdots \,, \qquad v = \varepsilon v_1 + \varepsilon^2 v_2 + \cdots \,,$$

$$p = p_1 + \varepsilon p_2 + \cdots \,, \qquad \psi = \varepsilon \psi_1 + \varepsilon^2 \psi_2 + \cdots \,, \tag{10}$$

$$h(\xi, \eta) = h_1(\xi)[1 + \varepsilon h_2(\xi)\zeta + \cdots] \,,$$

where $h_1(\xi)$ and $h_1(\xi)h_2(\xi)$ are the coefficients of a Taylor series of the elemental lengths h. Similar expansions would hold for $\bar{u}, \bar{v}, \bar{p}$ and $\bar{\psi}$ of the boundary layer around the cylinder $\eta = \eta_2$.

For the outer flow field we assume that

$$\Psi = \Psi_1 + \varepsilon \Psi_2 + \cdots \,, \tag{11}$$

and similar asymptotic expansions would hold for U, V and P. The expansions (10) and (11) are supposed to be derived from the same exact solution of the Navier–Stokes equations;

therefore they must match each other in the field where the three regions overlap. These matching conditions yield further boundary conditions for each expansion, and enable us to determine its successive terms alternately. It is easy to prove that the outer flow field is irrotational. Thus all Ψ_1, Ψ_2, . . . are solutions of the Laplace equation

$$\partial^2 \Psi / \partial \xi^2 + \partial^2 \Psi / \partial \eta^2 = 0 \ . \tag{12}$$

The boundary conditions for the outer solution are the conditions at infinity, and for the inner solutions they are the no-slip conditions on the two cylindrical surfaces. The additional boundary conditions required are obtained by means of Kaplun's matching technique.

Substituting (10) into (1), (2) and comparing like powers of ε we find the first-order equations:

$$\frac{\partial u_1}{\partial t} - \frac{\nu'(\cosh \eta_1 - \cos \xi)^2}{\sinh^2|\eta_1|} \frac{\partial^2 u_1}{\partial \zeta^2} = - \frac{\cosh \eta_1 - \cos \xi}{\sinh|\eta_1|} \frac{\partial p_1}{\partial \xi} \ , \tag{13}$$

$$\partial p_1 / \partial \zeta = 0 \ , \tag{14}$$

and the second-order equations:

$$\frac{\partial u_2}{\partial t} - \frac{\nu'(\cosh \eta_1 - \cos \xi)^2}{\sinh^2|\eta_1|} \frac{\partial^2 u_2}{\partial \zeta^2} = - \frac{\zeta \sinh \eta_1}{\sinh|\eta_1|} \frac{\partial p_1}{\partial \xi} - \frac{\cosh \eta_1 - \cos \xi}{\sinh|\eta_1|} \frac{\partial p_2}{\partial \xi}$$

$$- \frac{\cosh \eta_1 - \cos \xi}{\sinh|\eta_1|} \left(u_1 \frac{\partial u_1}{\partial \xi} + v_1 \frac{\partial u_1}{\partial \zeta} \right) + \frac{2 \nu' \zeta \sinh \eta_1 (\cosh \eta_1 - \cos \xi)}{\sinh^2|\eta_1|} \frac{\partial^2 u_1}{\partial \zeta^2} \ , \tag{15}$$

$$\partial p_2 / \partial \zeta = 0 \ . \tag{16}$$

Similar equations would hold for $\bar{u}_1$, $\bar{p}_1$ and for $\bar{u}_2$, $\bar{p}_2$. We notice that the first-order equations, (13) and (14), have the same form as the planar boundary layer equations. The second-order equations, (15) and (16), have extra terms which take the curvature into consideration. The boundary conditions are that the velocities on the two bodies are zero for each order and that the inner and outer solutions are matched by using intermediate variables.

At the initial stage, the boundary layers have not yet begun to grow. A potential flow prevails throughout the entire field, that is why Ψ_1 is just the stream function given in (6).

Noting that the pressure does not vary across the boundary layer around the cylinder $\eta = \eta_1$, we obtain the condition

$$\frac{\partial p_1}{\partial \xi} = \frac{\partial P_1}{\partial \xi} \bigg|_{\eta = \eta_1} = - \frac{\sinh|\eta_1|}{\cosh \eta_1 - \cos \xi} \frac{\partial U_1}{\partial t} \bigg|_{\eta = \eta_1} , \tag{17}$$

and the solution of (13).

Since $\psi_1 = 2\sqrt{\nu't} \int_0^{\tilde{\eta}} u_1 \, d\tilde{\eta}$, we have

$$\psi_1 = 2\sqrt{\nu't} U_{1|\eta = \eta_1} \left[\tilde{\eta} - \frac{\Gamma(\alpha + 1)}{2\Gamma(\alpha + \frac{3}{2})} + 2^{2\alpha} \Gamma(\alpha + 1) g_{\alpha + 1/2}(\tilde{\eta}) \right] , \tag{18}$$

where

$$\tilde{\eta} = \frac{\zeta}{2} \frac{\sinh|\eta_1|}{\sqrt{\nu' t}(\cosh\eta_1 - \cos\xi)}, \qquad g_\alpha(\tilde{\eta}) = \frac{2}{\sqrt{\pi}\Gamma(2\alpha+1)} \int_{\tilde{\eta}}^{\infty} (\gamma - \tilde{\eta})^{2\alpha} e^{-\gamma^2} d\gamma.$$

Similar solutions are obtained for the boundary layer around the cylinder $\eta = \eta_2$. For details see [23].

The expressions for Ψ_2, ψ_2 and $\bar{\psi}_2$ are obtained by applying the matching procedure. For example,

$$\Psi_2(\xi, \eta, t) = t^\alpha \sqrt{\nu' t} \frac{\Gamma(\alpha+1)}{\Gamma(\alpha+\frac{3}{2})} \left[\sum_{n=1}^{\infty} \frac{\sinh[n(\eta_2 - \eta)]}{\sinh[n(\eta_2 - \eta_1)]} \gamma_n \sin n\xi \right.$$
$$\left. - \sum_{n=1}^{\infty} \frac{\sinh[n(\eta_1 - \eta)]}{\sinh[n(\eta_1 - \eta_2)]} \bar{\gamma}_n \sin n\xi \right], \tag{19}$$

where γ_n and $\bar{\gamma}_n$ are known constants.

A uniformly valid solution for the stream function can be found by adding the outer and inner solutions and subtracting the matching terms.

4. Results and discussion

A primary aim of this paper is to find on the basis of the obtained formulae the initiation of boundary layer separation (detachment) and the drag force experienced on each cylinder as a function of the flow acceleration, the Reynolds number and the distance between the cylinders.

The decisive geometric characteristics of our study are the radii a and b of the cylinders and the distance d' between their centres. The other geometric parameters η_1, η_2 and focal separation c are defined through the following relations

$$\eta_1 = -\operatorname{arcosh} \frac{D'^2 + 1 - k^2}{2D'}, \qquad \eta_2 = \operatorname{arcosh} \frac{D'^2 + k^2 - 1}{2kD'},$$
$$c = -a \sinh\eta_1 = b \sinh\eta_2$$

where, see Fig. 1,

$$k = \frac{b}{a}, \qquad D = \frac{d}{a} \quad \text{and} \quad D' = \frac{d'}{a} = \frac{d+b+a}{a} = D + k + 1.$$

The study of the interaction between the viscous boundary layer and the outer inviscid flow has interested investigators because it is often necessary to know the distribution of skin friction and heat transfer across the interface of fluids and solids. The mechanism by which the outer flow feeds energy and momentum into the wake behind the blunt body is intimately connected with the phenomenon of separation. The aim of all analytical contributions in this area is to determine the point of separation. It is believed that the position of separation and the flow properties in its neighbourhood must be known before one can proceed to study and calculate the wake, containing coherent large-scale vortices in a relatively organized manner. If the amount of vorticity produced in the boundary layer at the

location of separation is known, then even inviscid theories could model successfully the wake [24]. In our theoretical investigation we follow the same ideology. We have obtained the solution of the problem formulated in Section 2 only for small times when the influence of the wake of the first cylinder on the flow around the second one is negligible. It is well known that up to now very little has been done to study analytically the properties of an unsteady (turbulent) wake made up of large-scale vortices. So for us the most interesting features of the flow for small times are: (i) the appearance of the point of zero skin friction which marks the onset of flow reversal, (ii) the hydrodynamic force interaction between the two cylinders.

4.1. Separation on the two cylindrical surfaces

The results obtained in the previous section have made it possible to examine the appearance of a point of zero skin friction, which marks the onset of the flow reversal. Setting the skin friction zero on the cylinders to the second order of approximation, we obtain:

$$\left(\frac{\partial u_1}{\partial \tilde{\eta}} + \varepsilon \frac{\partial u_2}{\partial \tilde{\eta}} \right) \bigg|_{\tilde{\eta}=0} = 0 , \tag{20}$$

$$\left(\frac{\partial \bar{u}_1}{\partial \tilde{\tilde{\eta}}} + \varepsilon \frac{\partial \bar{u}_2}{\partial \tilde{\tilde{\eta}}} \right) \bigg|_{\tilde{\tilde{\eta}}=0} = 0 . \tag{21}$$

The separation time T_{1S} on the two cylinders can be calculated from equations (20) and (21).

The distance covered by the fluid before detachment first takes place on each of the cylinders is given by

$$\sigma = \int_0^{t'} U_0 t^\alpha \, dt'/a = [(\nu' \, \mathrm{Re})^\alpha/(\alpha + 1)] T_{1S}^{\alpha+1} .$$

When $\alpha = 0$ we obtain $\sigma = T_{1S}$.

Some computations have been made to find out the dependence of the situation on (i) the Reynolds number Re, (ii) the separation distance D, (iii) the acceleration parameter α, and (iv) the ratio of the cylinder radii k.

Figure 2 shows the dependence of the initial-time boundary layer detachment on the Reynolds number Re for an impulsive ($\alpha = 0$) and a uniformly accelerated ($\alpha = 1$) flow
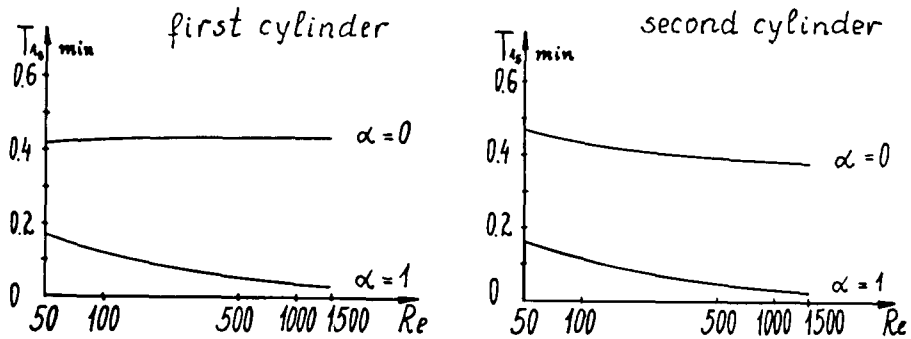

Fig. 2. Dependence of the initial-time boundary layer detachment on the Reynolds number for impulsive and uniformly accelerated flows around two cylinders.

around the cylinders. It is seen from this figure that in the case of the impulsive motion the detachment time changes slightly as the Reynolds number increase while in the case of accelerated motion the time at which detachment first appears is lessened strongly. We have drawn in Fig. 3 the graph of the dependence of the distance σ on the position (ξ) on the cylinder surfaces at Re = 100, $k = 1$, $D = 1.1$ and various values of the acceleration parameter α. The initial detachment time on the cylinder surfaces as a function of the separation distance D at Re = 1000, $\alpha = 0$ and various k are given in Fig. 4. One can observe that the influence of the separation distance on the detachment time is stronger on the first cylinder
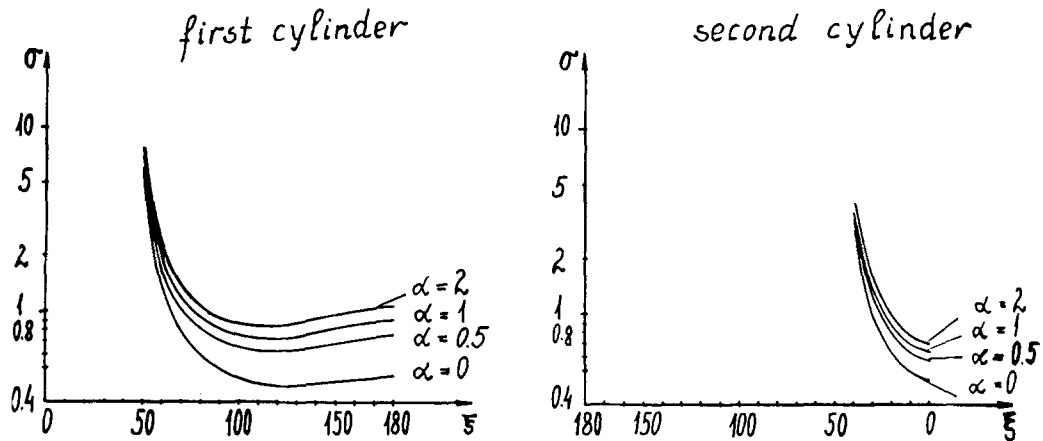

Fig. 3. Dependence of the distances σ on ξ at Re = 100, $k = 1$, $D = 1.1$ and various α.
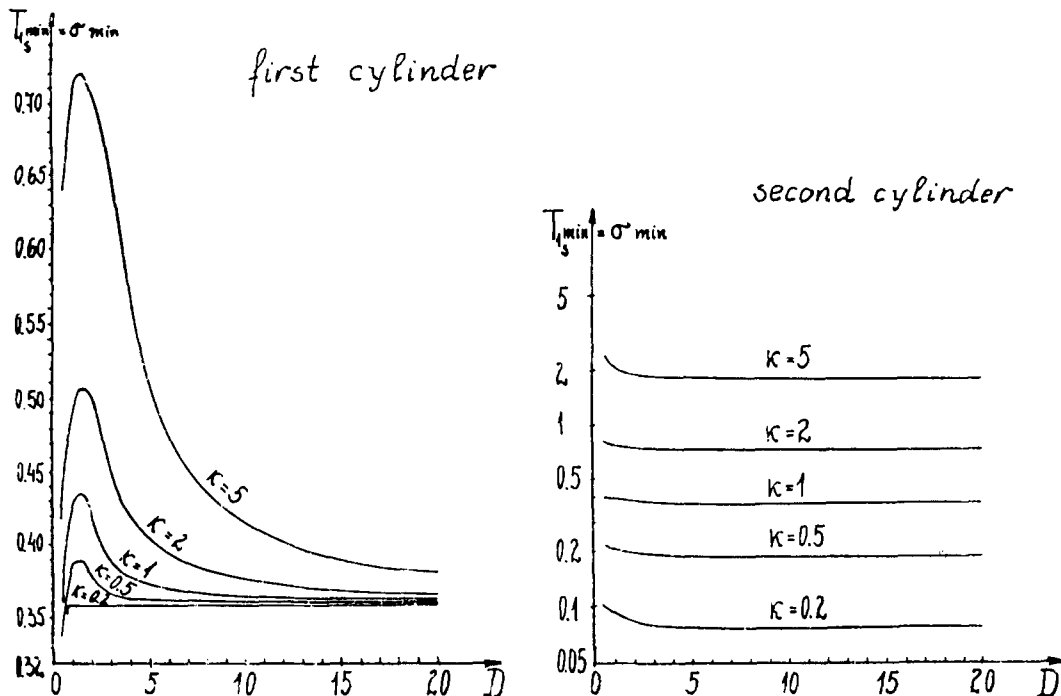

Fig. 4. Initial detachment time as a function of the separation distance D at Re = 1000, $\alpha = 0$ and various k.

than on the second one. We arrive also at the conclusion that the detachment time from the cylinders increases as the ratio of the cylinder radii k increases.

In Fig. 5 we present the streamline pattern for the first cylinder when the separation distance is very large, $D = 20$, and Re $= 100$, $k = 1$, $\alpha = 0$, $T_1 = 1$. For such D there is no difference at all between the streamline pattern around the first cylinder and around the second one. The comparison between the streamline pattern given in Fig. 5 with the streamline pattern obtained by Wang for a single circular cylinder under the same conditions shows a good coincidence (see Fig. 3 in [11]). This is so because Wang's solution for a single circular cylinder, under the same conditions, is a particular case of our solution for two circular cylinders when the separation distance D between them is very large.

Although our solution is based on the small-time assumption, qualitative results for large times are also obtained. Sure enough, for finite times, the first zero skin friction appears on the surface of the body to mark the onset of the flow reversal. It may be thought that the onset of reversed flow at once heralds the phenomenon of detachment in which the notion of a thin boundary layer embedded within an inviscid flow fails. Proudman and Johnson [25] demonstrate that this need not be the case. After the appearance of flow separation one can observe two recirculating bubbles behind each of the cylinders that are characterized by the points of detachment and reattachment on the two bodies. These bubbles are formed as a result of the convective non-linear terms in the Navier–Stokes equations. It is well known that a bubble is defined as a body of fluid contained in a closed steamline. A bubble is said to open or burst if the bounding contour opens, while retaining inside closed streamline loops. An interesting behavior is observed, at higher Reynolds numbers, that bubbles may burst unexpectedly.

4.2. Hydrodynamic force interaction

In order to investigate the hydrodynamic force interaction between the two cylinders it is necessary to calculate the integral effect of the hydrodynamic stresses acting upon each cylinder, which is equal to:
i) for the upstream cylinder

$$F_{x'1} = \int_0^{2\pi} \left(p_{12} \frac{\partial x'}{\partial \xi} + p_{22} \frac{\partial x'}{\partial \eta} \right) \bigg|_{\eta = \eta_1} d\xi , \tag{22}$$

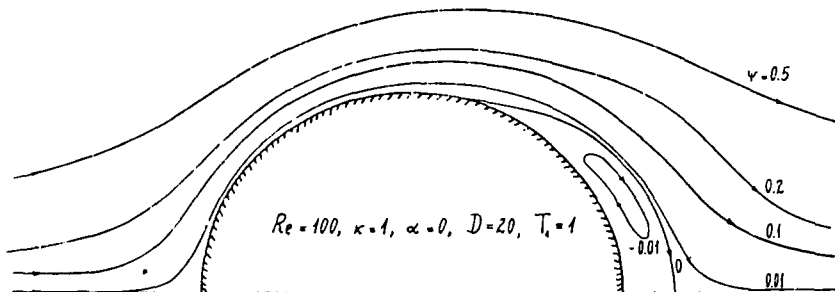ii) for the downstream cylinder

Fig. 5. Streamline pattern for two cylinders at $D = 20$, Re $= 100$, $k = 1$, $\alpha = 0$, $T_1 = 1$.

$$F_{x'2} = -\int_0^{2\pi} \left(p_{12} \frac{\partial x'}{\partial \xi} + p_{22} \frac{\partial x'}{\partial \eta} \right) \Big|_{\eta = \eta_2} \mathrm{d}\xi \ .$$ (23)

Here p_{12} and p_{22} are the tangential and normal components of the stress tensor.

After some algebra we have, from (22) and (23),

i) for the upstream cylinder

$$C_{D1} = \frac{F_{x'1}}{\rho U_0^2 \, \mathrm{St} \, a} = -\int_0^{2\pi} \left(\varepsilon \nu' \sinh \eta_1 \frac{\partial u_1}{\partial \zeta} \Big|_{\eta = \eta_1} + \sinh|\eta_1| \frac{\partial p_1}{\partial \xi} \Big|_{\eta = \eta_1} \right.$$

$$\left. + \sinh|\eta_1| \varepsilon \frac{\partial p_2}{\partial \xi} \Big|_{\eta = \eta_1} \right) \frac{\sin \xi}{\cosh \eta_1 - \cos \xi} \, \mathrm{d}\xi \ ,$$ (24)

ii) for the downstream cylinder

$$C_{D2} = \frac{F_{x'2}}{\rho U_0^2 \, \mathrm{St} \, a} = \int_0^{2\pi} \left(-\varepsilon \nu' \sinh \eta_2 \frac{\partial \bar{u}_1}{\partial \bar{\zeta}} \Big|_{\eta = \eta_2} + \sinh|\eta_1| \frac{\partial \bar{p}_1}{\partial \xi} \Big|_{\eta = \eta_2} \right.$$

$$\left. + \sinh|\eta_1| \varepsilon \frac{\partial \bar{p}_2}{\partial \xi} \Big|_{\eta = \eta_2} \right) \frac{\sin \xi}{\cosh \eta_2 - \cos \xi} \, \mathrm{d}\xi \ .$$ (25)

The hydrodynamic interaction force of the two cylinders depends strongly upon the values of the separation distance D. Figure 6 shows the drag coefficient of the two cylinders as a function of the separation distance D at Re = 100, $k = 1$, $\alpha = 0$ and various small values of time T_1. When the radii of the cylinders are equal and the times are small enough, in contrast to the steady flow past two circular cylinders [18], in the case of unsteady motion started from rest the drag coefficient of the downstream (second) cylinder is greater than the drag coefficient of the upstream (first) one. The explanation of this phenomenon is the
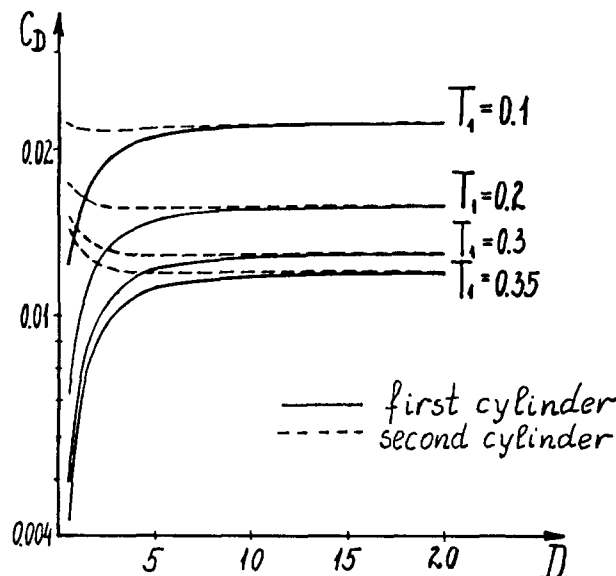

Fig. 6. Drag coefficients of two cylinders as a function of the separation distance D at Re = 100, $k = 1$, $\alpha = 0$ and different time T_1.

following. Since the initial condition (6) of the stream function represents the potential flow past two circular cylinders, the flow field of the viscous fluid is at first "inviscid". Due to the flow delaying behind the first cylinder, the velocity in front of the second cylinder is smaller than the velocity in front of the first one. So the pressure behind the first cylinder is greater than the pressure in front of it. That is why for very small times the drag coefficient of the downstream cylinder is greater than the drag coefficient of the upstream one. In the subsequent development of the flow the "viscous correction" increases quickly and one obtains the usual situation in which the drag coefficient of the first cylinder becomes greater than that of the second one. As can be expected, when the separation distance D tends to infinity, the drag coefficients of the two cylinders tend to that of a single circular cylinder under the same flow conditions.

The dependence of the drag coefficients of the two equal cylinders on the time T_1 and the separation distance D, for various values of the Reynolds number Re and the acceleration parameter α, are given in Figs 7 and 8 respectively. It is seen that the drag coefficients of the two cylinders decrease with increasing Reynolds number, and they increase with increasing acceleration parameter. The drag coefficient of the upstream cylinder is an increasing
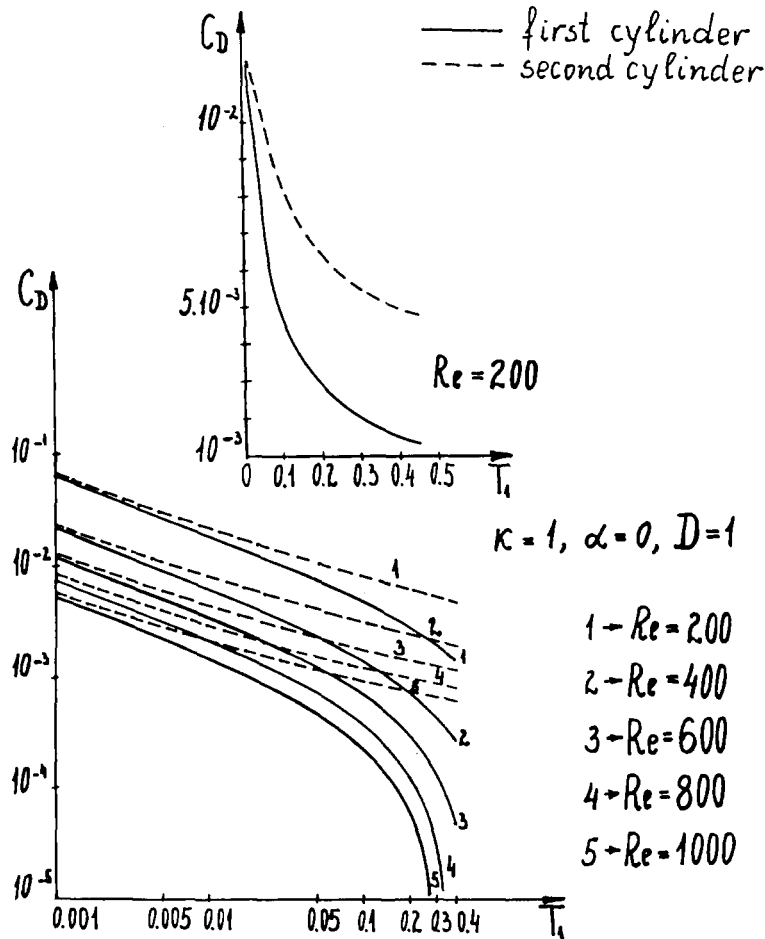

Fig. 7. Dependence of the drag coefficients of the two cylinders on the time T_1 at $k = 1$, $\alpha = 0$, $D = 1$ and different values of the Reynolds number.
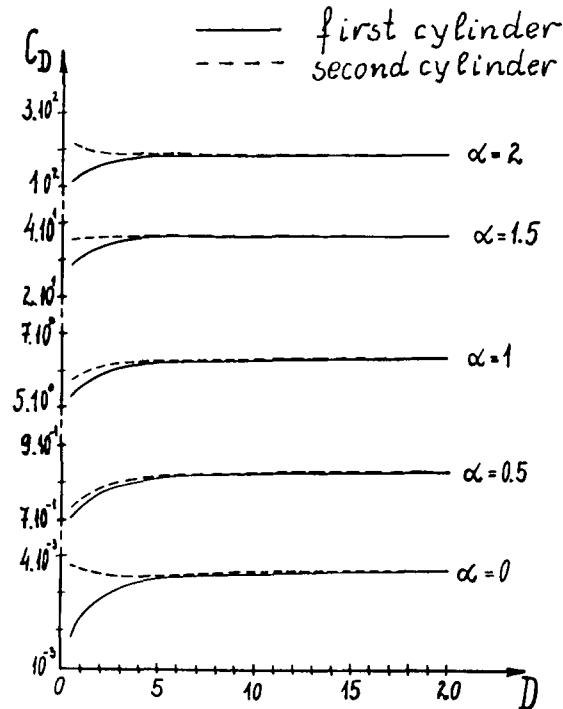
Fig. 8. Dependence of the drag coefficients of the two cylinders on the separation distance D for different values of the acceleration parameter α at $\mathrm{Re} = 500$, $k = 1$, $T_1 = 0.03$.

function of the separation distance D for all values of the acceleration parameter α. It is interesting to note that for small times and small separation distance D the dependence of the drag coefficient of the downstream cylinder on the acceleration parameter α is nonlinear. While for $\alpha = 0.5$, $\alpha = 1$, $\alpha = 1.5$ the drag coefficient of the downstream cylinder is an increasing function of the separation distance D, for $\alpha = 0$ and $\alpha = 2$ the drag coefficient of the downstream cylinder is a decreasing function of the separation distance D.

Figure 9 presents the drag coefficients of the two cylinders as a function of the time T_1 for various values of the ratio of the radii of two cylinders and $\mathrm{Re} = 500$, $\alpha = 0$, $D = 1$. The graphs 1, 2 and 3 in Fig. 9 show that when the radius of the second cylinder is equal to or greater than the radius of the first one, the difference between the drag coefficients of the second and the first cylinder increases with the increasing of the time T_1. When the radius of the second cylinder is smaller than the radius of the first one, the already mentioned difference decreases (graph 4 in Fig. 9) with the increasing of the time T_1.

In literature there are no results treating the unsteady interactions between two circular cylinders at small times. That is why we have compared our results in the limit case of large distance between the two bodies with the results in the case of one cylinder. Hence, in Fig. 10 we compare our results with Dennis and Staniforth's results [26] for the dependence of the quantity C_D St on the time T_1 at $D = 30$, $\alpha = 0$, $k = 1$ and various values of the Reynolds number. As can be seen from this figure the coincidence of the two results is excellent.

We note that unsteady separation responds with some inertia to an abrupt increase in the adverse pressure gradient. Applying the boundary layer equations we have specified the separation points in order to allow the continuation of the solution in terms of an appropriate wake model. In the dependence of the cylinder drag coefficients in unsteady
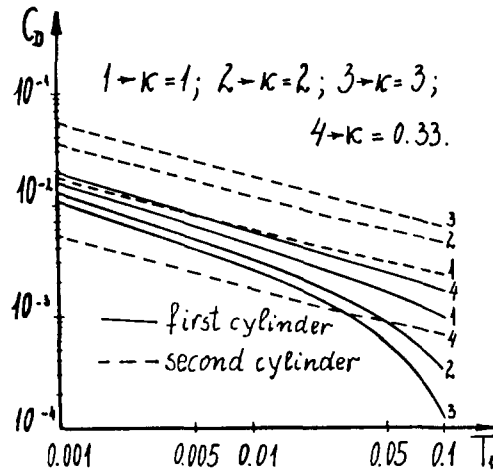
Fig. 9. Dependence of the drag coefficients on the time T_1 at Re = 500, $\alpha = 0$, $D = 1$ and various k.
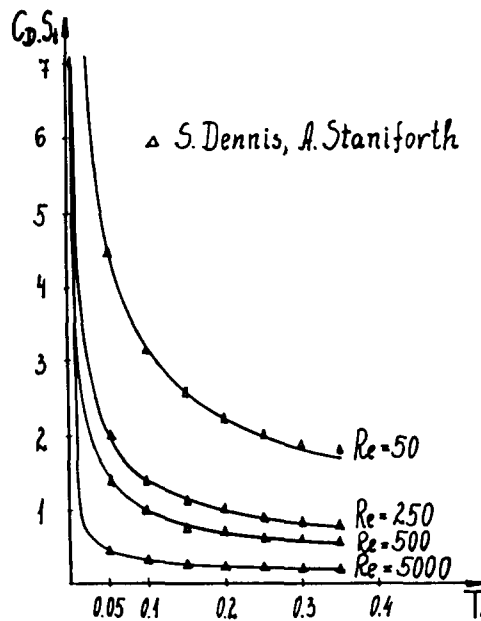

Fig. 10. Comparison of our results and Dennis and Staniforth's results for the dependence of the quantity C_D St on the time T_1 at $\alpha = 0$, $k = 1$, $D = 30$ and various values of the Reynolds number.

flows, viscosity plays a very significant role. It is due to shearing effects and their subsequent development into small- or large-scale turbulence.

5. Conclusions

After applying the method of matched asymptotic expansions we have obtained new results for the formation and initial stage of development of the boundary layers around two circular cylinders in a viscous flow with a velocity at infinity varying as some power of time. These

results generalize those concerning the single cylinder moving in an unbounded viscous fluid with the same velocity [10, 14]. The obtained approximate solution is valid for small times in the case when the flow at infinity is parallel to the plane containing the cylinders axes and perpendicular to these axes and for Reynolds number much larger than one, but small enough for the flow to remain stable.

It is shown that when the Reynolds number is large and the two equal cylinders are placed at large distance, the interaction between them fades away rapidly and the streamline pattern has the structure of the flow pattern for a single circular cylinder with the same radius and the same flow conditions. As the acceleration parameter increases, the times at which detachment first appears are reduced strongly, while as the Reynolds number increases the detachment times change weakly. The influence of the separation distance on the detachment times is stronger for the first cylinder than for the second one. In the case when the radii of the cylinders are different, the detachment times from them increase as the ratio of the cylinder radii k increases.

It should be mentioned that, in contrast to the steady flow past two circular cylinders, in the case of unsteady motion started from rest, the drag coefficient of the downstream cylinder for small times is greater than the drag coefficient of the upstream one. While the drag coefficient of the upstream cylinder is an increasing function of the separation distance for all values of the acceleration parameter, the drag coefficient of the downstream cylinder is an increasing function of the separation distance for some values of the acceleration parameter, and it is a decreasing function for the other values of the same parameter. The drag coefficient for both cylinders increases with increasing acceleration parameter.

Further we add that in the case of an impulsive motion the drag coefficient of each of the cylinders decreases with increasing Reynolds number. When the radius of the second cylinder is equal to or greater than the radius of the first one, the difference between the drag coefficients of the second and the first cylinder increases with increasing time. When the radius of the second cylinder is smaller than that of the first one, this difference decreases with increasing time.

Finally, we note that the scheme used for application of the method of inner and outer expansions for two-body hydrodynamic problems, appears to be capable to obtain many new relations and findings in the field of fluid mechanics.

References

1. Lord Rayleigh, On the motion of solid bodies through viscous liquids, *Philos. Mag.* 21 (1911) 697–711.
2. L. Howarth, Rayleigh's problem for a semi-infinite plate, *Proc. Cambridge Soc.* 46 (1950) 127–140.
3. H. Hasimoto, Note on Rayleigh's problem for a bent flat plate, *J. Phys. Soc. Japan* 6 (1951) 400–401.
4. L. Sowerby and J. Cooke, The flow of fluid along corners and edges, *Quart. Mech. Appl. Math.* 6 (1953) 50–70.
5. H.S. Carslaw and J.C. Jaeger, *The conduction of heat in solids*, Oxford University Press, Oxford, England (1947).
6. G.K. Batchelor, The skin friction on infinite cylinders moving parallel to their length, *Quart Mech. Appl. Math.* 7 (1954) 179–192.
7. H. Blasius, Grenzschichten in Flüssigkeiten mit kleiner Reibung, *Z. Math. Phys.* 56 (1908) 1–37.
8. S. Goldstein and L. Rosenhead, Boundary layer growth, *Proc. Cambr. Phil. Soc.* 32 (1936) 392–401.
9. H. Görtler, Verdrängungswirkung der laminaren Grenzschicht und Druckwiderstand, *Ing. Arch.* 14 (1944) 286–305.
10. E. Watson, Boundary layer growth, *Proc. Roy. Soc.* A231 (1955) 104–116.
11. C-Yi Wang, The flow past a circular cylinder which is started impulsively from rest, *J. Math. and Phys.* 46 (1967) 195–202.

12. C-Yi Wang, Separation and stall of an impulsively started elliptic cylinder, *J. Appl. Mech.* E34 (1967) 823–828.

13. Z. Zapryanov, Boundary layer growth around a parabolic cylinder, *Theory. and Appl. Mech.*, *BAS*, 2 (1974) 19–28.

14. Sl. Slavchev, Boundary layer growth on a circular cylinder, *Theor. and Appl. Mech.*, *Bas*, 4 (1975) 49–55.

15. Z.D. Zapryanov and P.G. Kalitzova-Kurteva, Boundary layer growth on a parabolic cylinder at angle of attack, *University Annual, Appl. Math.*, XII (1976), book 3, 185–194.

16. G. Simeonov, On the motion from rest of a class of cylinders. Elliptic cylinder case, *Theor. and Appl. Mech.*, *BAS*, 1 (1977) 64–75.

17. I.A. Belov, *Interaction of non-uniform flows with obstacles*, Mashinostroene, Leningrad (1983) (in Russian).

18. I.A. Belov and N.A. Kudriavtzev, Cross flow past two circular cylinders in line, (steady flow), *Journal of Physical Engineering* XLI (1981) 310–317.

19. S.S. Tabakova and Z. Zapryanov, On the hydrodynamic interaction of two spheres oscillating in a viscous fluid. I: Axisymmetrical case, *ZAMP* 33 (1982) 344–357.

20. S.S. Tabakova and Z. Zapryanov, On the hydrodynamic interaction of two spheres oscillating in a viscous fluid. II: Three dimensional case, *ZAMP* 33 (1982) 487–502.

21. D.P. Telionis, *Unsteady viscous flows*, Springer-Verlag, New York, Heidelberg, Berlin (1981).

22. J. Happel, H. Brenner, *Low Reynolds number hydrodynamics*, Prentice-Hall (1965).

23. P.G. Kalitzova-Kurteva, Hydrodynamic interaction in unsteady viscous flow past two bodies, Ph.D. Thesis, Univ. of Sofia (1987).

24. S.F. Shen, Unsteady separation according to the boundary-layer equation. In: *Adv. Appl. Mech.*, ed. C.S. Yih: 18 (1978) 177–220.

25. I. Proudman and K. Johnson, Boundary layer growth near a rear stagnation point, *J. Fluid Mech.* 12 (1962) 161–168.

26. S.C.R. Dennis and A.N. Staniforth, A numerical method for calculating the initial flow past a cylinder in a viscous fluid, *Lecture Notes in Physics* 8 (1970) 343–349.